doi:10.1016/S0022-2836(02)00466-7 available online at http://www.idealibrary.com on IDEAL® J. Mol. Biol. (2002) 320, 159–164

JMB

COMMUNICATION

The Cytochrome *c* Folding Landscape Revealed by Electron-transfer Kinetics

Jennifer C. Lee, I-Jy Chang, Harry B. Gray* and Jay R. Winkler*

Beckman Institute, California Institute of Technology Pasadena, CA 91125, USA

**Corresponding authors*

We have investigated the folding energy landscape of cytochrome *c* by exploiting the widely different electron-transfer (ET) reactivities of buried and exposed Zn(II)-substituted hemes. An electronically excited Zn-porphyrin in guanidine hydrochloride denatured Zn-substituted cytochrome *c* (Zn-cyt *c*) reduces ruthenium(III) hexaammine about ten times faster than when embedded in the fully folded protein. Measurements of ET kinetics during Zn-cyt *c* folding reveal a burst intermediate in which one-third of the ensemble has a protected Zn-porphyrin and slow ET kinetics; the remaining fraction exhibits fast ET characteristic of a solvent-exposed redox cofactor. The ET data show that, under solvent conditions favoring the folded protein, collapsed non-native structures are not substantially more stable than extended conformations, and that the two populations interchange rapidly. Most of the folding free energy, then, is released when compact structures evolve into the native fold.

Keywords: protein folding; cytochrome *c*; electron transfer; burst intermediate

Great strides have been made recently in understanding exactly how a polypeptide self-assembles into the native structure of a protein.[1–11] Energy landscape models, in particular, have provided a conceptual framework that has aided both the design and interpretation of folding experiments.[12,13] The configurational entropy of a polypeptide, represented by the lateral dimension on a funnel-shaped folding energy landscape, is minimized at the native conformation. This unfavorable configurational entropy change is balanced by a decrease in enthalpy due to native-contact formation, and an increase in solvent entropy.[1] It is the large change in configurational entropy that can introduce mechanistic (and, in turn, kinetics) complexity. Without detailed maps of the folding energy landscape, it is uncertain at what stage the conformational heterogeneity of the unfolded ensemble is lost. This issue is difficult to resolve experimentally; folding probes must report not just the average progress of the unfolded ensemble toward the folded state, but on the ensemble heterogeneity as well. Indeed, few spectroscopic methods can even distinguish between single and bimodal distributions of molecules in a partially folded ensemble.

The reactivity of a polypeptide can be an extremely sensitive indicator of structural heterogeneity. With a carefully selected probe reaction, a bimodal distribution of protein conformations would exhibit biphasic kinetics, whereas a single-mode distribution would react in a single phase. The key requirement is that the probe reaction be fast compared to the time scale of folding ($<10^{-4}$ to $>10^{1}$ seconds). Electron-transfer (ET) reactions could be excellent folding probes because rates at high driving forces are determined by the distance and medium separating the two redox partners.[14] Buried redox centers in proteins often exchange electrons rather slowly with reagents in solution. Unfolding will greatly increase the accessibility of a redox cofactor and can lead to much faster ET. Compact intermediates might be expected to exhibit ET rates somewhere between those of the folded and unfolded molecules.

Present address: I.-Jy. Chang, National Taiwan Normal University, Taipei, Taiwan, ROC.

Abbreviations used: ET, electron transfer; cyt *c*, cytochrome *c*; GuHCl, guanidine hydrochloride; CD, circular dichroism.

E-mail addresses of the corresponding authors: hbgray@caltech.edu; winklerj@caltech.edu

0022-2836/02/$ - see front matter

We have investigated the folding landscape of Zn(II)-substituted cytochrome *c* (Zn-cyt *c*)[15] with ET reactivity probes. Zn-cyt *c* is structurally homologous to the native protein (Fe-cyt *c*), which has been studied in great detail.[11,16–18] A non-native axial ligand (His26 or His33) replaces Met80 at neutral pH in denatured horse heart Fe-cyt *c*;[19] the rate-limiting folding step in this case is correction of heme misligation. Owing to weaker binding and faster substitution at the sixth coordination site, replacement of Fe with Zn will eliminate axial ligand traps during refolding.[20] The key advantage of the Zn-substituted protein is the availability of a long-lived (~15 ms), powerfully reducing ($E^0 = -0.8$ V *versus* NHE) triplet excited state (*Zn-cyt *c*), which can be prepared in 90% yield[21] with 580 nm laser excitation.[22]

Equilibrium unfolding of Zn-cyt *c*

Addition of guanidine hydrochloride (GuHCl) to solutions of Zn-cyt *c* produces a blue shift in the Soret absorption band (folded, $\lambda_{max} = 426$ nm; unfolded, $\lambda_{max} = 418$ nm), giving a species with a spectrum similar to that of Zn(II)-substituted myoglobin ($\lambda_{max} = 414$ nm).[23] GuHCl unfolding curves generated from Soret absorption and far-UV CD spectra show that the stability of folded Zn-cyt *c* is comparable to that of the Fe(III) form (Fe(III): $\Delta G_f^0 = -40(1)$ kJ mol^{-1}, $[GuHCl]_{1/2} = 2.8(1)$ M; Zn(II): $\Delta G_f^0 = -35(2)$ kJ mol^{-1}, $[GuHCl]_{1/2} = 2.9(1)$ M).[24,25] In contrast to Fe-cyt *c*, the Zn center in the unfolded protein should not be ligated by any peptide side-chain other than the native His18.[20]

Triplet-excited Zn-cyt *c* is quenched by $Ru(NH_3)_6^{3+}$, producing Zn-cyt *c*$^{+}$ and $Ru(NH_3)_6^{2+}$ (Figure 1, inset). The reported quenching rate constant measured under native conditions is 1.4×10^7 M^{-1} s^{-1}.[22] Moderate concentrations of GuHCl (<1.0 M) do not unfold the protein, but accelerate $Ru(NH_3)_6^{3+}$ quenching, presumably because of the increased ionic strength.[26] Under denaturing conditions ([GuHCl] > 3 M), the quenching reaction is 100 times faster (1.4×10^9 M^{-1} s^{-1}, [GuHCl] = 3.5 M) than that measured in the absence of GuHCl. At a GuHCl concentration corresponding to the midpoint of Zn-cyt *c* unfolding (2.85 M), the $Ru(NH_3)_6^{3+}$ quenching kinetics are biexponential. Both rate constants exhibit a linear dependence on $[Ru(NH_3)_6^{3+}]$, giving respective values of 7.2×10^7 and 1.0×10^9 M^{-1} s^{-1} for folded and unfolded ensembles (Figure 1). The latter quenching rate is very high, owing to the greater accessibility of the Zn-porphyrin in the unfolded protein. The *Zn-cyt *c* ET kinetics are generally consistent with a two-state unfolding process. The unfolding isotherm generated from ET kinetics exhibits a transition midpoint at 2.8(1) M GuHCl, in good agreement with those obtained from far-UV CD and heme absorption measurements (Figure 1).

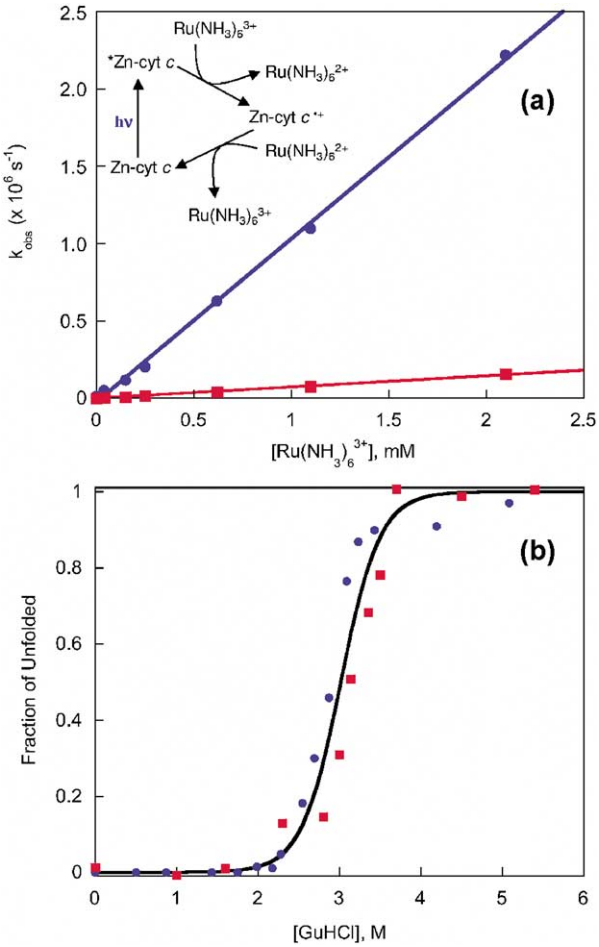

Figure 1. (a) ET quenching of *Zn-cyt *c* by $Ru(NH_3)_6^{3+}$ (inset: reaction scheme) in deoxygenated denaturant solution (2.85 M GuHCl, 100 mM sodium phosphate, pH 7). The *Zn-cyt *c* decay under these conditions is biexponential and both observed rate constants vary linearly with $[Ru(NH_3)_6^{3+}]$. The second-order rate constants extracted from these measurements are attributed to bimolecular ET reactions of folded (7.2×10^7 M^{-1} s^{-1}, red squares) and unfolded (1.0×10^9 M^{-1} s^{-1}, blue circles) protein. (b) Denaturation curve for Zn-cyt *c* generated from Soret absorption (red squares) and ET rate (blue circles) data. Zn-cyt *c* was prepared from commercial horse heart protein according to standard procedures.[15] Guanidine hydrochloride and $[Ru(NH_3)_6]Cl_3$ were from commercial sources and used without additional purification.

Zn-cyt *c* folding kinetics

Changes in Zn-cyt *c* Soret absorption (418 and 426 nm) after stopped-flow dilution of denaturant (initial [GuHCl] = 3.4 M; final [GuHCl] = 1.20–2.60 M) were examined: the transient absorption kinetics are exponential functions and the observed rate constants depend linearly on denaturant concentration, decreasing from $1.3(\pm 0.2) \times 10^2$ s^{-1} at 1.20 M GuHCl to $1.1(\pm 0.1) \times 10^1$ s^{-1} at 2.60 M GuHCl. The extrapolated time constant for refolding in the absence of denaturant is about a millisecond. The Zn-cyt *c* folding rate is about ten

times higher than that of the Fe(III) protein at comparable driving forces,[11,16] consistent with the absence of heme misligation.

More complex Zn-cyt *c* folding becomes apparent when the process is probed with transient absorption measurements (450 nm) of *Zn-cyt *c*/$Ru(NH_3)_6^{3+}$ ET kinetics. As the polypeptide chain folds around the porphyrin, the *Zn-cyt *c* ET rate decreases from its value in the unfolded protein ($\sim 7 \times 10^6\ s^{-1}$, $[Ru(NH_3)_6^{3+}] = 3–5$ mM) to that characteristic of folded molecules ($\sim 2.5 \times 10^5\ s^{-1}$). Biphasic *Zn-cyt *c* decay kinetics are observed during protein refolding; biexponential functions provide adequate fits to the *Zn-cyt *c* kinetics, although the residuals suggest that more than just two decay components are present. Fits to the kinetics recorded 1 ms after GuHCl dilution to 1.46 M reveal that two-thirds of the excited Zn-porphyrins decay in a fast phase ($7(\pm 2) \times 10^6\ s^{-1}$) attributable to largely unfolded protein; the remaining third exhibits a rate constant ($3.5(\pm 1.5) \times 10^5\ s^{-1}$) closer to that expected for folded molecules. ET kinetics measured at longer folding times remain biphasic with the amplitude of the faster component decreasing in favor of an increase in the amplitude of the slow component (Figure 2).

Both rate constants extracted from biexponential fits to the *Zn-cyt *c* decay kinetics decrease by about a factor of 2 as the folding reaction proceeds (1 ms, $7(\pm 2) \times 10^6$, $3.5(\pm 1.5) \times 10^5\ s^{-1}$; 50 ms, $3(\pm 2) \times 10^6$, $2.2(\pm 0.4) \times 10^5\ s^{-1}$) (Figure 2). This variation in quenching efficiency, although close to the uncertainties in our measured rate constants, may reflect a gradual collapse of polypeptide structures during folding. It is important to note, however, that biexponential functions only approximate the *Zn-cyt *c* decay kinetics. It is likely that the two rate constants extracted from these fits represent the average ET rates of two heterogeneous populations of polypeptides, one largely unfolded, the other compact. In this case, the shifts in *Zn-cyt *c* decay constants could reflect subtle changes in the composition of these two groups during protein folding.

The amplitudes of the two *Zn-cyt *c* decay phases vary exponentially with folding time and the rate constant ($33\ s^{-1}$, [GuHCl] = 1.46 M) is in reasonable agreement with that measured by Soret absorption spectroscopy. It is noteworthy that, at the earliest measured folding times (1 ms), there are significant amplitudes in both the fast and slow *Zn-cyt *c* ET phases (~67% fast; ~33% slow). This is substantially more than would be expected on the basis of the stopped-flow dead-time (~1 ms) and the observed rate constants extracted from the signal amplitudes. Measurements of *Zn-cyt *c* kinetics at different GuHCl concentrations consistently extrapolate back to a "burst-phase" ensemble[11,16,27,28] with a 2:1 ratio of fast and slow ET components (Figure 3): these results demonstrate that the burst ensemble is heterogeneous; molecules in one-third of the protein population have compact structures, and those in the remaining fraction have exposed Zn-porphyrins.

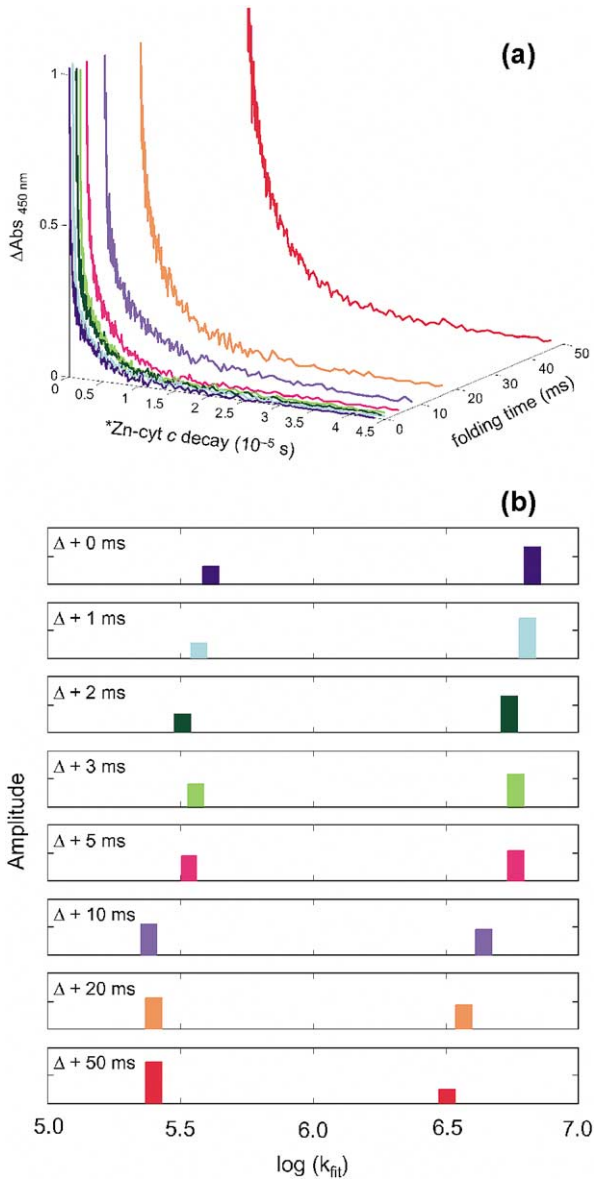

Figure 2. Zn-cyt *c* folding probed by ET kinetics. (a) Folding initiated by stopped-flow denaturant dilution (final concentrations: [GuHCl] = 1.46 M; [Zn-cyt *c*] = 10 μM; $[Ru(NH_3)_6^{3+}] = 4$ mM; pH 7) and monitored by laser transient absorption measurements of *Zn-cyt *c* decay (450 nm, signals normalized to an initial value of 1.0) at different delay times after mix was complete (0, 1, 2, 3, 5, 10, 20, and 50 ms). (b) Rate constants and relative amplitudes from biexponential fits of *Zn-cyt *c* decay data measured during protein folding. The observed rate constants decrease by about a factor of 2 as folding proceeds. Protein folding was initiated using a stopped-flow mixer with a calculated mixing deadtime (Δ) of ~1 ms. ET kinetics were measured during Zn-cyt *c* folding by synchronizing pulsed laser excitation with the stopped-flow mixer. Data from ten laser shots ([Zn-cyt *c*] = 10 μM; one laser shot per mix) provided adequate signal-to-noise levels.

It is apparent that there is underlying complexity in Zn-cyt *c* folding. The fraction of the burst

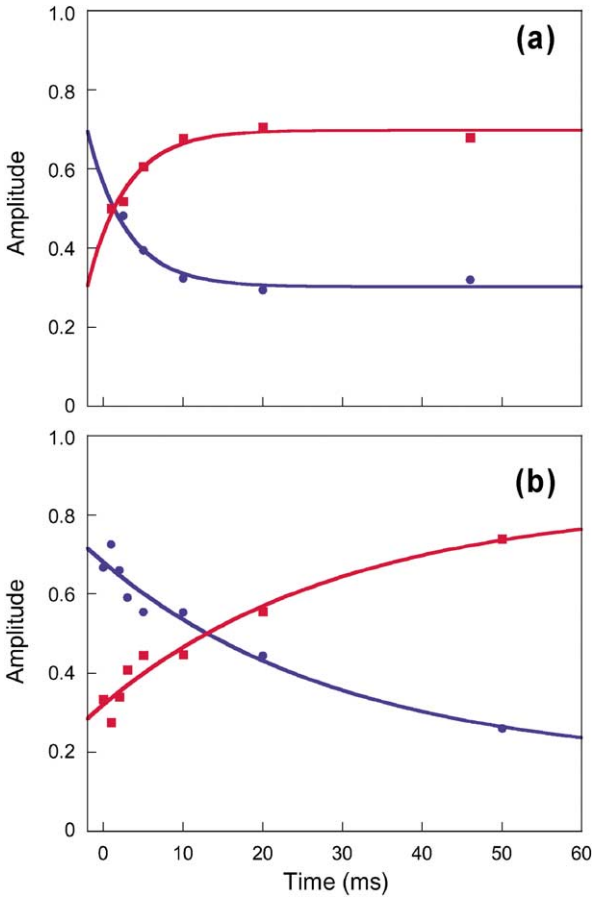

Figure 3. Amplitudes of fast and slow decay constants extracted from biexponential fits to *Zn-cyt *c* decay kinetics as functions of time after the initiation of protein folding. The amplitudes vary exponentially with folding time and extrapolate to a ~2:1 fast:slow ratio at time zero. (a) Final [GuHCl] = 1.10 M, folding rate constant, $k_{fold} = 200\ s^{-1}$; (b) final [GuHCl] = 1.46 M, $k_{fold} = 33\ s^{-1}$.

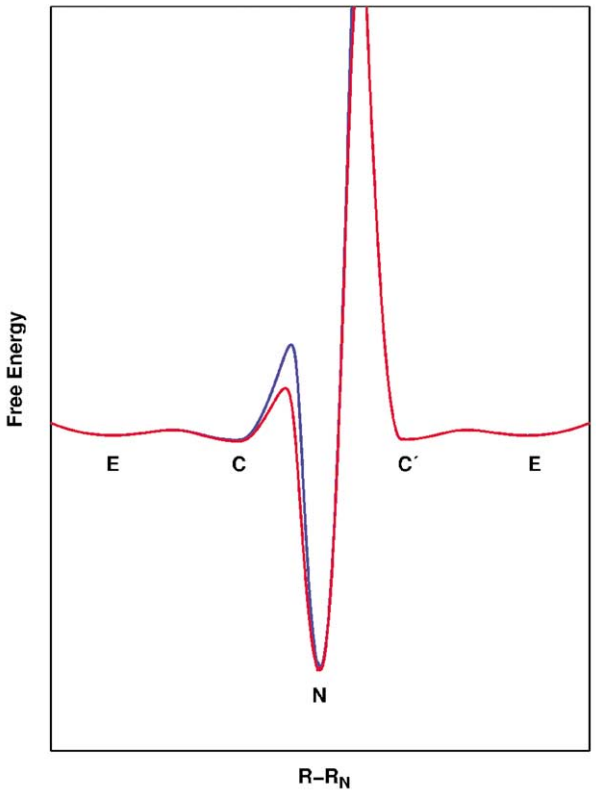

Figure 4. Qualitative folding energy profile for cytochrome *c* as a function of the deviation of the protein radius (R) from its value in the native fold (R_N). Extended (E) and compact (C) structures are nearly degenerate and equilibrate on a submillisecond time scale. Compact structures fold in the Fe protein by crossing an energy barrier (blue curve) with a sizable ligand-substitution component. There is no ligand substitution barrier for folding from the compact structures of the Zn protein (red curve). Topologically trapped compact structures (C′) must extend and collapse to a productive structure (C) in order to reach the native conformation (N).

ensemble (~1/3) with slow *Zn-cyt *c* decay kinetics could be fully folded protein or an ensemble of compact non-native structures. The former possibility would be an example of "fast-track" folding,[29–31] where about a third of the unfolded Zn-cyt *c* molecules adopt conformations that can refold very quickly. The remaining protein molecules have relatively exposed porphyrin groups, and fold on a substantially longer time scale. Alternatively, the 2:1 ratio of fast/slow *Zn-cyt *c* decay components formed immediately after dilution of [GuHCl] may reflect a shift in the equilibrium between unfolded and compact non-native structures. Although it is often assumed that native solvent conditions will strongly favor compact structures, the *Zn-cyt *c* ET kinetics clearly indicate that two-thirds of the molecules in the burst intermediates have highly exposed porphyrins. Ultimately, the entire protein ensemble folds because, at low [GuHCl], the native structure is much more stable than unfolded conformations.

A strikingly similar picture of the cytochrome *c* folding landscape has emerged from an analysis of fluorescence energy-transfer kinetics during refolding of a dansyl-labeled native protein.[32] Compact non-native structures of Fe-cyt *c* appear within the stopped-flow mixing time, long before the native protein is formed at pH 7.[33] By analogy, we suggest that the compact structures formed immediately after denaturant dilution with Zn-cyt *c* are non-native conformations. For both Zn-cyt *c* and Fe-cyt *c*, compact non-native and extended polypeptide conformations are populated during the formation of fully folded molecules. These observations accord with theoretical analyses by Shakhnovich and co-workers that have shown that extended and compact structures could be in equilibrium under folding conditions.[34,35]

The schematic folding energy profile derived from our measurements on cytochrome *c* (Figure 4) suggests that nearly degenerate extended (E) and compact (C) structures equilibrate rapidly (<1 ms) after denaturant is diluted. Compact structures in the Fe protein can fold by crossing

an energy barrier that has a substantial ligand-substitution component. This barrier is lowered in the Zn protein because there is no misligation.[20] Owing to topological frustration, not all collapsed conformations (C') can proceed to folded product.[30] Molecules that fall into these topological traps must re-extend ($C' \rightarrow E$) in order to form productive collapsed species (C). Rapid equilibration between quasi-degenerate collapsed and extended populations facilitates this error-correction process. The energy landscape that can be inferred from these cyt *c* folding studies has a vast number of extended structures that rapidly exchange with one another and with compact intermediates. Low energy barriers separate the productive compact structures on this surface from the deep energy well of the native fold.

Acknowledgments

J.C.L. thanks the Ralph M. Parsons Foundation for a graduate fellowship. I.J.C. gratefully acknowledges financial support from the National Taiwan Normal University and the National Science Council of the Republic of China. This research was supported by the National Science Foundation (MCB-997477, DBI-9876443) and the Arnold and Mabel Beckman Foundation.

References

1. Onuchic, J. N., Nymeyer, H., Garcia, A. E., Chahine, J. & Socci, N. D. (2000). The energy landscape theory of protein folding: insights into folding mechanisms and scenarios. *Advan. Protein Chem.* **53**, 87–152.
2. Portman, J. J., Takada, S. & Wolynes, P. G. (2001). Microscopic theory of protein folding rates. I. Fine structure of the free energy profile and folding routes from a variational approach. *J. Chem. Phys.* **114**, 5069–5081.
3. Portman, J. J., Takada, S. & Wolynes, P. G. (2001). Microscopic theory of protein folding rates. II. Local reaction coordinates and chain dynamics. *J. Chem. Phys.* **114**, 5082–5096.
4. Özkan, S. B., Bahar, I. & Dill, K. A. (2001). Transition states and the meaning of phi-values in protein folding kinetics. *Nature Struct. Biol.* **8**, 765–769.
5. Mirny, L. & Shakhnovich, E. I. (2001). Protein folding theory: from lattice to all-atom models. *Annu. Rev. Biophys. Biomol. Struct.* **30**, 361–396.
6. Kazmirski, S. L., Wong, K. B., Freund, S. M. V., Tan, Y. J., Fersht, A. R. & Daggett, V. (2001). Protein folding from a highly disordered denatured state: the folding pathway of chymotrypsin inhibitor-2 at atomic resolution. *Proc. Natl Acad. Sci. USA*, **98**, 4349–4354.
7. Wong, K. B., Clarke, J., Bond, C. J., Neira, J. L., Freund, S. M. V., Fersht, A. R. & Daggett, V. (2000). Towards a complete description of the structural and dynamic properties of the denatured state of barnase and the role of residual structure in folding. *J. Mol. Biol.* **296**, 1257–1282.
8. Eaton, W. A., Munoz, V., Hagen, S. J., Jas, G. S., Lapidus, L. J., Henry, E. R. & Hofrichter, J. (2000). Fast kinetics and mechanisms in protein folding. *Annu. Rev. Biophys. Biomol. Struct.* **29**, 327–359.
9. Kuwata, K., Shastry, R., Cheng, H., Hishino, M., Batt, C. A., Goto, Y. & Roder, H. (2001). Structural and kinetic characterization of early folding events in beta-lactoglobulin. *Nature Struct. Biol.* **8**, 151–155.
10. Jager, M., Nguyen, H., Crane, J. C., Kelly, J. W. & Gruebele, M. (2001). The folding mechanism of a beta-sheet: the WW domain. *J. Mol. Biol.* **311**, 373–393.
11. Englander, S. W., Sosnick, T. R., Mayne, L. C., Shtilerman, M., Qi, P. X. & Bai, Y. (1998). Fast and slow folding in cytochrome *c*. *Acc. Chem. Res.* **31**, 737–744.
12. Bryngelson, J. D., Onuchic, J. N. & Wolynes, P. G. (1995). Funnels, pathways and the energy landscape of protein folding—a synthesis. *Proteins: Struct. Funct. Genet.* **21**, 167–195.
13. Dill, K. A. & Chan, H. S. (1997). From Levinthal to pathways to funnels. *Nature Struct. Biol.* **4**, 10–19.
14. Gray, H. B. & Winkler, J. R. (1996). Electron transfer in proteins. *Annu. Rev. Biochem.* **65**, 537–561.
15. Vanderkooi, J. M., Landesberg, R., Hayden, G. & Owen, C. S. (1977). Metal-free and metal-substituted cytochromes *c*. Use in characterization of the cytochrome *c* binding site. *Eur. J. Biochem.* **81**, 339–347.
16. Shastry, M. C. R., Sauder, J. M. & Roder, H. (1998). Kinetic and structural analysis of submillisecond folding events in cytochrome *c*. *Acc. Chem. Res.* **31**, 717–725.
17. Hagen, S. J., Hofrichter, J. & Eaton, W. A. (1997). Rate of intrachain diffusion of unfolded cytochrome *c*. *J. Phys. Chem. B*, **101**, 2352–2365.
18. Pierce, M. M. & Nall, B. T. (1997). Fast folding of cytochrome *c*. *Protein Sci.* **6**, 618–627.
19. Colón, W., Wakem, L. P., Sherman, F. & Roder, H. (1997). Identification of the predominant non-native histidine ligand in unfolded cytochrome *c*. *Biochemistry*, **36**, 12535–12541.
20. Scheidt, W. R., Kastner, M. E. & Hatano, K. (1978). Sterochemistry of the toluene solvate of α,β,γ,δ-tetraphenylporphinatozinc(II). *Inorg. Chem.* **17**, 706–710.
21. Sudha, B. P., Dixit, N., Moy, V. T. & Vanderkooi, J. M. (1984). Reactions of excited-state cytochrome *c* derivatives. Delayed fluorescence and phosphorescence of zinc, tin, and metal-free cytochrome *c* at room temperature. *Biochemistry*, **23**, 2103–2107.
22. Elias, H., Chou, M. H. & Winkler, J. R. (1988). Electron-transfer kinetics of Zn-substituted cytochrome *c* and its $Ru(NH_3)_5$(histidine-33) derivative. *J. Am. Chem. Soc.* **110**, 429–434.
23. Cowan, J. A. & Gray, H. B. (1989). Synthesis and properties of metal-substituted myoglobins. *Inorg. Chem.* **28**, 2074–2078.
24. Mines, G. A., Pascher, T., Lee, S. C., Winkler, J. R. & Gray, H. B. (1996). Cytochrome *c* folding triggered by electron transfer. *Chem. Biol.* **3**, 491–497.
25. Tezcan, F. A. (2001). Reactions of heme proteins in solutions and crystals. PhD thesis, California Institute of Technology.
26. Wherland, S. & Gray, H. B. (1976). Metalloprotein electron transfer reactions: analysis of reactivity of horse heart cytochrome *c* with inorganic complexes. *Proc. Natl Acad. Sci. USA*, **73**, 2950–2954.
27. Akiyama, S., Takahashi, S., Ishimori, K. & Morishima, I. (2000). Stepwise formation of α-helices during cytochrome *c* folding. *Nature Struct. Biol.* **7**, 514–520.

28. Sauder, J. M. & Roder, H. (1998). Amide protection in an early folding intermediate of cytochrome *c*. *Fold. Des.* **3**, 293–301.
29. Zhou, Y. & Karplus, M. (1999). Folding of a model three-helix bundle protein: a thermodynamic and kinetic analysis. *J. Mol. Biol.* **293**, 917–951.
30. Thirumalai, D., Klimov, D. K. & Woodson, S. A. (1997). Kinetic partitioning mechanism as a unifying theme in the folding of biomolecules. *Theor. Chem. Acc.* **96**, 14–22.
31. Mirny, L. A., Abkevich, V. & Shakhnovich, E. I. (1996). Universality and diversity of the protein folding scenarios: a comprehensive analysis with the aid of a lattice model. *Fold. Des.* **1**, 103–116.
32. Lyubovitsky, J. G., Gray, H. B. & Winkler, J. R. (2002). Mapping the cytochrome *c* folding landscape. *J. Am. Chem. Soc.* **124**, 5481–5485.
33. Sosnick, T. R., Mayne, L., Hiller, R. & Englander, S. W. (1994). The barriers in protein folding. *Nature Struct. Biol.* **1**, 149–156.
34. Finkelstein, A. V. & Shakhnovich, E. I. (1989). Theory of cooperative transitions in protein molecules. II. Phase diagram for a protein molecule in solution. *Biopolymers*, **28**, 1681–1694.
35. Gutin, A. M., Abkevich, V. I. & Shakhnovich, E. I. (1995). Is burst hydrophobic collapse necessary for protein folding? *Biochemistry*, **34**, 3066–3076.

Edited by C. R. Matthews

(Received 20 December 2001; received in revised form 3 May 2002; accepted 8 May 2002)